Molecular and Functional Characterization of GABA Receptor Subunits GRD and LCCH3 from Human Louse Pediculus Humanus Humanus

Omar Hashim, Claude L. Charvet, Berthine Toubaté, Aimun A.E. Ahmed, Nicolas Lamassiaude, Cédric Neveu, Isabelle Dimier-Poisson, Françoise Debierre-Grockiego, Catherine Dupuy

1521-0111/102/2/116–127$35.00
Molecular Pharmacology

dx.doi.org/10.1124/molpharm.122.000499
Mol Pharmacol 102:116–127, August 2022

Molecular and Functional Characterization of GABA Receptor Subunits GRD and LCCH3 from Human Louse *Pediculus Humanus Humanus*[S]

Omar Hashim, Claude L. Charvet, Berthine Toubaté, Aimun A.E. Ahmed, Nicolas Lamassiaude, Cédric Neveu, Isabelle Dimier-Poisson, Françoise Debierre-Grockiego, and Catherine Dupuy

INRAE, Université de Tours, ISP, BioMAP, 37200, Tours, France (O.H., B.T., I.D.-P., F.D.-G., C.D.); Department of Pharmacology, Faculty of Pharmacy, University of Gezira, Wad Madani, Sudan (O.H.); INRAE, Université de Tours, ISP, MPN, 37380, Nouzilly, France (C.L.C., N.L., C.N.); Department of Pharmacology, Albaha University, Alaqiq, Saudi Arabia (A.A.E.A.); and Department of Pharmacology and Toxicology, Omdurman Islamic University, Omdurman, Sudan (A.A.E.A.)

Received February 5, 2022; accepted May 12, 2022

ABSTRACT

Human louse *Pediculus humanus* is a cosmopolitan obligatory blood-feeding ectoparasite causing pediculosis and transmitting many bacterial pathogens. Control of infestation is difficult due to the developed resistance to insecticides that mainly target GABA (γ-aminobutyric acid) receptors. Previous work showed that *Pediculus humanus humanus* (Phh) GABA receptor subunit resistance to dieldrin (RDL) is the target of lotilaner, a synthetic molecule of the isoxazoline chemical class. To enhance our understanding of how insecticides act on GABA receptors, two other GABA receptor subunits were cloned and characterized: three variants of *Phh-grd* (glycine-like receptor of *Drosophila*) and one variant of *Phh-lcch3* (ligand-gated chloride channel homolog 3). Relative mRNA expression levels of *Phh-rdl*, *Phh-grd*, and *Phh-lcch3* revealed that they were expressed throughout the developmental stages (eggs, larvae, adults) and in the different parts of adult lice (head, thorax, and abdomen). When expressed individually in the *Xenopus* oocyte heterologous expression system, Phh-GRD1, Phh-GRD2, Phh-GRD3, and Phh-LCCH3 were unable to reconstitute functional channels, whereas the subunit combinations Phh-GRD1/Phh-LCCH3, Phh-GRD1/Phh-RDL, and Phh-LCCH3/Phh-RDL responded to GABA in a concentration-dependent manner. The three heteromeric receptors were similarly sensitive to the antagonistic effect of picrotoxin and fipronil, whereas Phh-GRD1/Phh-RDL and Phh-LCCH3/Phh-RDL were respectively about 2.5-fold and 5-fold more sensitive to ivermectin than Phh-GRD1/Phh-LCCH3. Moreover, the heteropentameric receptor constituted by Phh-GRD1/Phh-LCCH3 was found to be permeable and highly sensitive to the extracellular sodium concentration. These findings provided valuable additions to our knowledge of the complex nature of GABA receptors in human louse that could help in understanding the resistance pattern to commonly used pediculicides.

SIGNIFICANCE STATEMENT

Human louse is an ectoparasite that causes pediculosis and transmits several bacterial pathogens. Emerging strains developed resistance to the commonly used insecticides, especially those targeting GABA receptors. To understand the molecular mechanisms underlying this resistance, two subunits of GABA receptors were cloned and described: *Phh-grd* and *Phh-lcch3*. The heteromeric receptor reconstituted with the two subunits was functional in *Xenopus* oocytes and sensitive to commercially available insecticides. Moreover, both subunits were transcribed throughout the parasite lifecycle.

Introduction

Human louse (*Pediculus humanus*, order *Phthiraptera*) is a cosmopolitan obligatory blood-feeding ectoparasite. There are two main ecotypes of human louse with nearly identical genomes (Olds et al., 2012): the head louse *Pediculus humanus capitis* causing pediculosis, a major public health concern, and the body louse *Pediculus humanus humanus* (Phh), transmitting *Rickettsia prowazekii* responsible for epidemic typhus, *Borellia recurrentis* responsible for relapsing fever, and *Bartonella quintana* causing trench fever (Badiaga and

This work was supported by Campus France [N° 934152H] (to O.H.), the Ministry of Higher Education-Sudan and the University of Gezira-Sudan (to O.H. and A.A.E.A.), the Université of Tours (to B.T., I.D.-P., F.D.-G., and C.D.), the INRAE (to C.L.C. and C.N.), and the Fédération de Recherche en Infectiologie of the Region Centre Val-de-Loire (to C.L.C. and C.D.).
No author has an actual or perceived conflict of interest with the contents of this article.
dx.doi.org/10.1124/molpharm.122.000499.
[S] This article has supplemental material available at molpharm.aspetjournals.org.

ABBREVIATIONS: aa, amino acids; bp, base pairs; CDS, coding sequence; Ct, cycle threshold; E, exon; GluCl, glutamate chloride; GRD, glycine-like receptor of *Drosophila*; LCCH3, ligand-gated chloride channel homolog 3; LGIC, ligand-gated ion channel; nACh, nicotinic acetylcholine; ORF, open reading frame; PCR, polymerase chain reaction; Phh, *Pediculus humanus humanus*; qPCR, quantitative PCR; RACE, rapid amplification of cDNA ends; RDL, resistance to dieldrin; RT-PCR, reverse transcription PCR; TEVC, two-electrode voltage-clamp; TM, transmembrane; TSS, transcription starting site; UTR, untranslated region.

Brouqui, 2012; Amanzougaghene et al., 2020). Historically, massive epidemics of relapsing fever and of typhus have affected Africa and Eurasia, and these diseases have recently reemerged in Europe by travelers and increasing numbers of refugees from endemic regions (Bechah et al., 2008; Hoch et al., 2015; Wilting et al., 2015; Antinori et al., 2016; Osthoff et al., 2016; Hytönen et al., 2017; DE LA Filia et al., 2018).

Chemical insecticides were widely applied to eliminate human louse, leading to emergence of strains resistant to the most commonly used pediculicides such as carbaryl (carbamates), pyrethrin (pyrethroids), and ivermectin (Clark et al., 2013; Amanzougaghene et al., 2020; Mohammadi et al., 2021). Furthermore, the use of organochlorides (lindane) was prohibited due to high toxicity to humans and the environment (Sangaré et al., 2016). Deciphering the mechanisms of action of insecticides on human louse could help to prevent resistance. To this end, laboratory-reared human body louse is a good model, since the individuals of the colony have never been exposed to chemical products and have not developed resistance.

Pentameric transmembrane Cys-loop ligand-gated ion channels (LGICs) are the major pharmacological targets of insecticides (Tong et al., 2021). Among them, γ-aminobutyric acid (GABA) receptors are traditional drug targets for organochlorides (dieldrin), phenylpyrazoles (fipronil), picrotoxin, and the macrocyclic lactones (ivermectin). GABA receptors of insects share common molecular features: long N-terminal extracellular domain constituting the GABA binding site, Cys-loop motif of 13 amino acids (aa), and four transmembrane domains (TM1–TM4) forming the pore of the ion channel with TM2 containing the molecular determinants of ion selectivity (Kozuska and Paulsen, 2012). In human cells, hundreds of combinations of GABA receptor subunits exist, leading to highly variable conductance for different ions, activation/desensitization times, and GABA EC_{50} (concentration required to mediate 50% of the maximum current in electrophysiology assay). The activity of human GABA receptors is modulated by different agonists and antagonists like benzodiazepines or barbiturates (Sallard et al., 2021). Because of this diversity, it has been shown that ivermectin is not toxic for humans (Johnson-Arbor, 2022).

Four subunits of GABA receptors have been described in insects: resistance to dieldrin (RDL), glycine-like receptor of *Drosophila* (GRD), ligand-gated chloride channel homolog 3 (LCCH3), and CG8916 (Buckingham et al., 2005). Among them, the genes encoding GRD and LCCH3 subunits were identified in *Drosophila melanogaster* (Harvey et al., 1994), *Laodelphax striatellus* (Wei et al., 2017), *Chilo suppressalis* (Jia et al., 2019; Huang et al., 2021), *Apis mellifera* (Henry et al., 2020), and *Blattella germanica* (Jones et al., 2021). Although GRD and LCCH3 did not form functional homomeric channels, their coexpression reconstituted heteropentameric cationic selective channel in *D. melanogaster, A. mellifera*, and *Varroa destructor* (Gisselmann et al., 2004; Ménard et al., 2018; Henry et al., 2020). In human louse, we recently characterized Phh-RDL that constituted a homopentameric anion-selective receptor with higher affinity to lotilaner (isoxazoline) and lower affinity to ivermectin (Lamassiaude et al., 2021). However, the functionality of GRD and LCCH3 has never been investigated in the order *Phthiraptera*.

In this explorative study, the molecular characterization of the two GABA receptor subunits Phh-GRD and Phh-LCCH3 is reported for the first time. The relative expression levels of *Phh-grd*, *Phh-lcch3*, and *Phh-rdl* were assayed in different parts and throughout the developmental stages of human body louse. Moreover, the functional expression and pharmacological characterization of the heteropentameric receptors constituted by Phh-GRD1/Phh-RDL, Phh-LCCH3/Phh-RDL, and Phh-GRD1/Phh-LCCH3 in response to GABA, picrotoxin, fipronil, and ivermectin were investigated.

Materials and Methods

Reagents. All reagents are of molecular biology grade. Chemicals including GABA, acetylcholine, glutamate, glycine, aspartate, histamine, serotonin, picrotoxin, fipronil, and ivermectin were purchased from Sigma-Aldrich (Saint-Quentin-Fallavier, France). GABA, acetylcholine, glutamate, glycine, aspartate, histamine, and serotonin were directly dissolved in the recording solution, whereas picrotoxin, fipronil, and ivermectin were first prepared at 10 mM DMSO and then diluted in recording solution to the final concentrations in which DMSO did not exceed 0.1%.

Isolation of RNA and Synthesis of First Strand cDNA. Human body lice were reared in the BioMAP laboratory as previously described (Lamassiaude et al., 2021). Total RNA was extracted from 30 mg of adult lice using NucleoSpin RNA plus extraction kit (Macherey-Nagel, Hoerdt, France) according to the manufacturer's instructions. For RACE (rapid amplification of cDNA ends)-PCR (polymerase chain reaction), the cDNA ends were amplified from 5 μg of RNA using Gene Racer kit (Invitrogen, Thermo Fisher Scientific, Courtaboeuf, France) according to the manufacturer's instructions. Each 5′ and 3′ RACE-PCR was performed with gene-specific primers and nested gene-specific primers binding to a site at short distance apart (Fig. 1; Table 1). The thermal cycling conditions were 94°C for 5 minutes, then 35 cycles of 94°C for 30 seconds, 58°C for 30 seconds, and 72°C for 1 minute and final extension at 72°C for 5 minutes. For reverse transcription PCR (RT-PCR), 0.5 μg of RNA was reverse transcribed with a mixture of oligo dT and 5′ RACE-PCR gene-specific primers and the superscript III reverse transcriptase (Invitrogen). Full-length *Phh-grd* and *Phh-lcch3* transcripts were amplified using 1 μl of cDNA and 10 pmol of two gene-specific primers (Table 1) using GoTaq DNA Polymerase (Promega, Charbonnières-les-Bains, France) according to the manufacturer's instructions. After migration on agarose gel, the PCR products were purified using Nucleo Spin Gel and PCR clean-up kit (Macherey-Nagel) according to the manufacturer's instructions. All RACE-PCR, RT-PCR and PCR products were cloned in pGEM-T Easy Vector (Promega) and sequenced by Eurofins Genomics (Ebersberg, Germany).

Sequence Analysis and Phylogeny. All cloned sequences were compared with the putative sequences deposited in Vector Base with Geneious Software (Biomatters, Auckland, New Zealand) and Basic Local Alignment Search Tool (BLAST; U.S. National Library of Medicine, Bethesda, MD) (https://blast.ncbi.nlm.nih.gov/Blast.cgi). Deduced amino acid sequences of full-length Phh-GRD and Phh-LCCH3 were obtained from ExPASy translate (Swiss Institute of Bioinformatics, Lausanne, Switzerland) (https://web.expasy.org/translate/); signal peptide cleavage sites were predicted using the SignalP 5.0 server (DTU Health Tech, Lyngby, Denmark, https://services.healthtech.dtu.dk/service.php?SignalP-5.0) (Petersen et al., 2011); and transmembrane domains were identified using the TMHMM program (https://services.healthtech.dtu.dk/service.php?TMHMM-2.0). Multiple sequence alignments were done by Clustal Omega algorithm (www.clustal.org/omega/) (Madeira et al., 2019), then viewed and annotated by Jalview software (https://www.jalview.org/). All aa sequences of GABA receptor subunits of *A. mellifera*: Am-GRD (NP_001292813.1), Am-LCCH3 (XP_026298403.1), Am-RDL (AJE68941); *D. melanogaster*: Dm-GRD (NP_524131.1), Dm-LCCH3 (NP_996469.1), Dm-RDL (NP_523991), *L. striatellus*: Ls-GRD (KX355313), Ls-LCCH3 (KX355312), Ls-RDL (BAF31884.1); *Nasonia vitripennis*: Nv-GRD (NP_001234887.1), Nv-LCCH3 (NP_001234895.1); *Tribolium castaneum*:

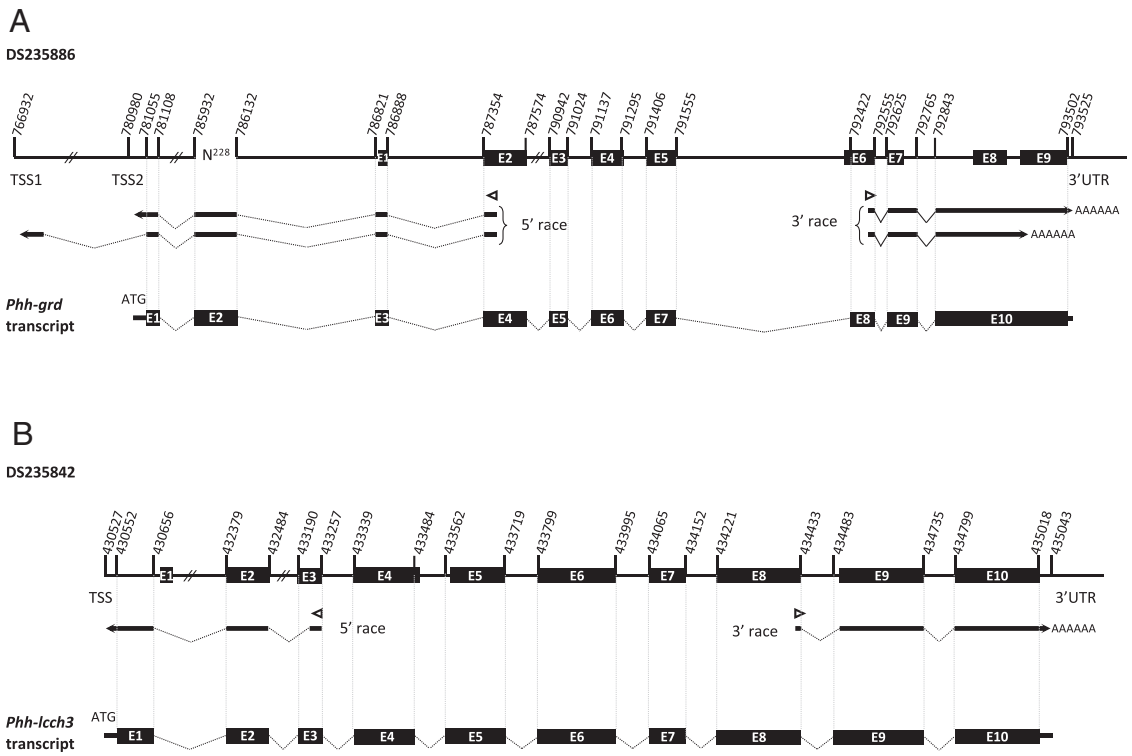

Fig. 1. Genomic and transcript organization of *Phh-grd* (A) and *Phh-lcch3* (B). Exons are represented by black boxes in expanded views of the contigs DS235886 with the annotated *Phh-grd* CDS (A, top drawing) and DS235842 with the annotated *Phh-lcch3* CDS (B, top drawing). The numbers indicated on DS235886 and DS235842 correspond to the final annotation of the genes. Positions of the primers are indicated by white arrows; 5′ and 3′ extremities are indicated by black arrows. On the bottom drawings are shown the final organizations of the *Phh-grd* (A) and *Phh-lcch3* (B) transcripts.

Tc-GRD (XP_015834304.1), Tc-LCCH3 (NP_001103251.1), Tc-RDL (NP_001107809.1); and *V. destructor*: Vd-GRD (KY748054.1), Vd-LCCH3 (KY748055.1), Vd-RDL (KY748050.1), and Phh-RDL (QRX-38896.1) were obtained from the National Center for Biotechnology Information (NCBI) database (https://www.ncbi.nlm.nih.gov). The phylogenetic tree was constructed by Molecular Evolutionary Genetics Analysis Version 7.0 (MEGA7) software (https://www.megasoftware.net/) (Kumar et al., 2016) using the Neighbor-Joining method, and the bootstrap values were calculated on 1050 replicates. The evolutionary distances were computed using the Poisson correction method and are in the units of the number of aa substitutions per site. Phh-β1, a subunit of nicotinic acetylcholine (nACh) from human louse, was used as an out-group to root the tree.

Expression Vector Cloning and Synthesis of cRNA. The full-length *Phh-grd* variants and *Phh-lcch3* were amplified using GoTaq polymerase (Promega) and cloned in the pTB207 expression vector using the In-Fusion HD Cloning Kit (Takara Bio Europe SAS, Saint-Germain-en-Laye, France) as described (Lamassiaude et al., 2021). Recombinant plasmids were purified using E.Z.N.A. Plasmid DNA Mini Kit (Omega Bio-Tek, Inc., Norcross, GA), and correct cloning was confirmed by sequencing (Eurofins Genomics). cRNAs were obtained from plasmids linearized by Msc1 (Thermo Fisher Scientific) using mMessage mMachine T7 transcription kit (Thermo Fisher Scientific) following the manufacturer's instructions. cRNA concentrations were measured by spectrophotometry (NanoDrop; Thermo Fisher Scientific), and integrity of cRNAs was confirmed by running

TABLE 1
Primers used for 5′ RACE, 3′ RACE, and amplification of full-length *Phh-grd* and *Phh-lcch3*

Primers	Sequences (5′-3′)
Phh-grd 5′ RACE first PCR	CGAAATCGGGCCCATGCTTC
Phh-grd 5′ RACE nested PCR	CGGGCCCATGCTTCGTACC
Phh-grd 3′ RACE first PCR	GACTTTATCAAGATGGACGAGTTC
Phh-grd 3′ RACE nested PCR	GGACGAGTTCTTTATTCCAGC
Phh-grd full forward	ATTTTCCGTGGTGGAATTTTTTTTC
Phh-grd full Xho1 forward[a]	*CTGGCGGCCGCTCGAG*ATGGCGTCGATGTTCGGA
Phh-grd full reverse	GAATACATAGTAAAAATAAATAAAT
Phh-grd full Apa1 reverse[a]	GAATACATAGTAAAAATAAATAAAT*GGGCCCGAGCTTGATCTGGT*
Phh-lcch3 5′ RACE first PCR	CGTTGTCGTGAAACGCATACC
Phh-lcch3 5′ RACE nested PCR	TTTCAGCAAAATCACCCGCC
Phh-lcch3 full Xho1 forward[a]	*CTGGCGGCCGCTCGAG*GGAATGATGATGCAATGCAGC
Phh-lcch3 full Apa1 reverse[a]	GCAATGAGTAGTAAATATTTATAC*GGGGCCCGAGCTTGATCTGGT*

[a]Primers Xho1 and Apa1 were designed with extensions (in italic) for recombination with the expression vector PTB207 linearized by Xho1 and Apa1.

500 ng in 1% agarose gel in TAE buffer (40 mM Tris-acetate–1 mM EDTA).

Quantitative PCR. Total RNA extraction and cDNA synthesis were done as described in section "Isolation of RNA and synthesis of first strand cDNA" from 30 mg of nits, L1, L2, and L3 larvae stages, as well from heads, thoraxes, and abdomens of adult lice. Applying comparative cycle threshold (Ct) experiment $2^{-(\Delta Ct)}$, 100 ng of cDNA was added to 10 μl of SYBR Green Master Mix (Thermo Fisher Scientific) and 10 pmol of gene-specific primers (Table 2) in a final volume of 20 μl. The quantitative PCR (qPCR) was performed with primary denaturation at 95°C for 10 minutes followed by 40 cycles of 95°C for 15 seconds and 60°C for 1 minute using the StepOnePlus Real-Time PCR System (Applied Biosystems, Thermo Fisher Scientific) following the conditions recommended by the manufacturer. Actin was used as endogenous control, and a melt curve cycle (95°C for 15 seconds, 60°C for 1 minute, and 95°C for 15 seconds) was added to confirm specific amplification.

Functional Expression and Pharmacology of Receptors. Defolliculated oocytes of *Xenopus laevis* (Ecocyte Bioscience, Dortmund, Germany) were injected individually with 30 ng of cRNA of *Phh-grd1,Phh-grd2*, *Phh-grd3*, *Phh-lcch3*, *Phh-rdl*, *Phh-grd1/Phh-lcch3*, *Phh-grd2/Phh-lcch3, Phh-grd3/Phh-lcch3*, *Phh-grd1/Phh-rdl*, or *Phh-lcch3/Phh-rdl* using a Drummond Nanoject II Microinjector (Dominique Dutscher SAS, Bernolsheim, France) and maintained for 3–5 days at 19°C in incubation solution (100 mM NaCl, 2 mM KCl, 1.8 mM $CaCl_2.2H_2O$, 1 mM $MgCl_2.6H_2O$, 5 mM HEPES, and 2.5 mM $C_3H_3NaO_3$ at pH 7.5 with 100 U/ml penicillin and 100 μg/ml streptomycin). Two-electrode voltage-clamp (TEVC) was used to measure currents generated by the application of increasing concentrations of GABA (0.3, 1, 3, 10, 30, 100, and 300 μM in recording solution: 100 mM NaCl, 2.5 mM KCl, 1 mM $CaCl_2.2H_2O$, and 5 mM HEPES at pH 7.3). The membrane potential was clamped at −60 mV and current signals were recorded with an oocyte clamp OC-725C amplifier (Warner Instruments, Holliston, MA) and analyzed by pCLAMP 10.4 Software (Molecular Devices, San Jose, CA). Normalized peak current amplitudes were plotted against the corresponding concentrations of GABA. Acetylcholine, glutamate, glycine, aspartate, histamine, and serotonin were tested at 30 μM on Phh-GRD1/Phh-LCCH3 to verify its specificity for GABA. To analyze the ion selectivity of the channel constituted by Phh-GRD1/Phh-LCCH3, reverse potential-ion concentration relationship was obtained by applying voltage ramps (−60 mA to +60 mA) in the presence of 100 μM GABA using recording solution with decreasing concentrations of Na^+ (100, 75, 50, 25, 12.5, and 0 mM) by the replacement of NaCl with tetra-ethyl ammonium chloride. The change in reversal potential was plotted against the concentrations of sodium.

The effect of antagonists (10 μM picrotoxin, 1 μM fipronil, or 1 μM ivermectin) was evaluated on Phh-RDL, Phh-GRD1/Phh-LCCH3, Phh-GRD1/Phh-RDL, and Phh-LCCH3/Phh-RDL by preincubation of each antagonist alone for 90 seconds followed by their coapplication with 100 μM GABA for 10 seconds. The observed responses were normalized to the response induced by 100 μM GABA alone performed before challenging with the antagonist.

Statistical Analysis. Statistical comparisons were performed with Prism 7 (GraphPad Software, Inc., San Diego, CA) using one-way ANOVA test followed by Tukey's multiple comparisons test. The sample size and the number of experiments were determined according to the previous results on Phh-RDL (Lamassiaude et al., 2021). A power of the test >80% was calculated a posteriori with a statistical tool of AnaStats (https://www.anastats.fr/) when differences were observed between the groups. The study is explorative and the *P* values are descriptive.

Results

Identification of *Phh-grd* and *Phh-lcch3* Transcripts. Using tBLASTn with *Apis mellifera, Am-grd* (NM_001305884.1), and *Am-lcch3* (NM_001077812.1) as query against the whole genome sequence of *P. humanus humanus* in VectorBase, *Phh-grd* (XM_002433141.1; PHUM 616750) and *Phh-lcch3* (XM_002430956.1; PHUM 507170) subunit genes located respectively in the super contigs DS235886 and DS235842 were identified. The coding sequences (CDSs) of 1272 bp (base pairs) for *Phh-grd* and 1404 bp for *Phh-lcch3* are organized in 9 and 10 exons (E) encoding proteins of 423 aa and 467 aa, respectively. Confusingly, no signal peptide is annotated on the putative protein sequence of both subunits.

To characterize 5′ and 3′ ends of *Phh-grd* and *Phh-lcch3*, RACE-PCR was done on total RNA extracted from adult lice using primers binding to the putative E2 (5′) and E6 (3′) of *Phh-grd* and E3 (5′) and E8 (3′) of *Phh-lcch3* (Fig. 1). For *Phh-grd* 5′ RACE, two transcription start sites (TSSs) were identified at positions 766932 and 780980 (Fig. 1A). In both cases, the transcripts have the same 5′ end organization: an extension of 29 bp in the 5′ direction of the annotated E1 (becoming E3) and two extra 5′ exons of 198 bp (E2) and 54 bp (E1). It is important to note that in the transcribed E2, 162 bp did not match with the genome of human body louse. Indeed, at the genomic level, these 162 bp are located in a stretch of undefined nucleotides, suggesting a mistake in sequencing/assembly of the whole genome (Fig. 1A; N^{228}). Results of 3′ RACE of *Phh-grd* revealed two possible sites for the end of transcripts after and inside putative exon 9. These alternative transcripts were found in many clones and further confirmed by results of transcriptomics (unpublished data). The RACE-PCR result of *Phh-lcch3* showed a modified position of E1 (Fig. 1B), including single TSS at position 430552 and single end of transcript at position 435043. Differences were observed in the lengths of putative and transcribed E4 (27 nucleotides shorter), E5 (26 nucleotides longer), and E9 (61 nucleotides longer) (Fig. 1B).

Based on the sequence analysis of RACE-PCR products, primers were designed to amplify and clone three full-length coding sequences of *Phh-grd* (*Phh-grd1, Phh-grd2*, and *Phh-grd3*) and one full-length coding sequence of *Phh-lcch3*. *Phh-grd* transcripts were 1869 bp, including a 5′ untranslated region

TABLE 2
Primers designed for qPCR for *Phh-grd*, *Phh-lcch3*, *Phh-rdl*, and *β-actin*

Primers	Sequences (5′-3′)	Amplicon Sizes (bp)
Phh-grd forward	GGTTTGGAAGCAAGAACGGAC	155
Phh-grd reverse	CCGAAATAACATTCACCCGAACCG	
Phh-lcch3 forward	GGGTATAACCACGGTACTAAC	171
Phh-lcch3 reverse	CTTGCTCCCCAATATGTATAG	
Phh-rdl forward	GCGAAAAAGTAGATTTATGGCG	174
Phh-rdl reverse	GTACCTCCTTTGGAATGAGC	
β-actin forward	TGCCACATGCTATTCTCCGT	60
β-actin reverse	CGGCAGTGGTAGTGAATGAA	

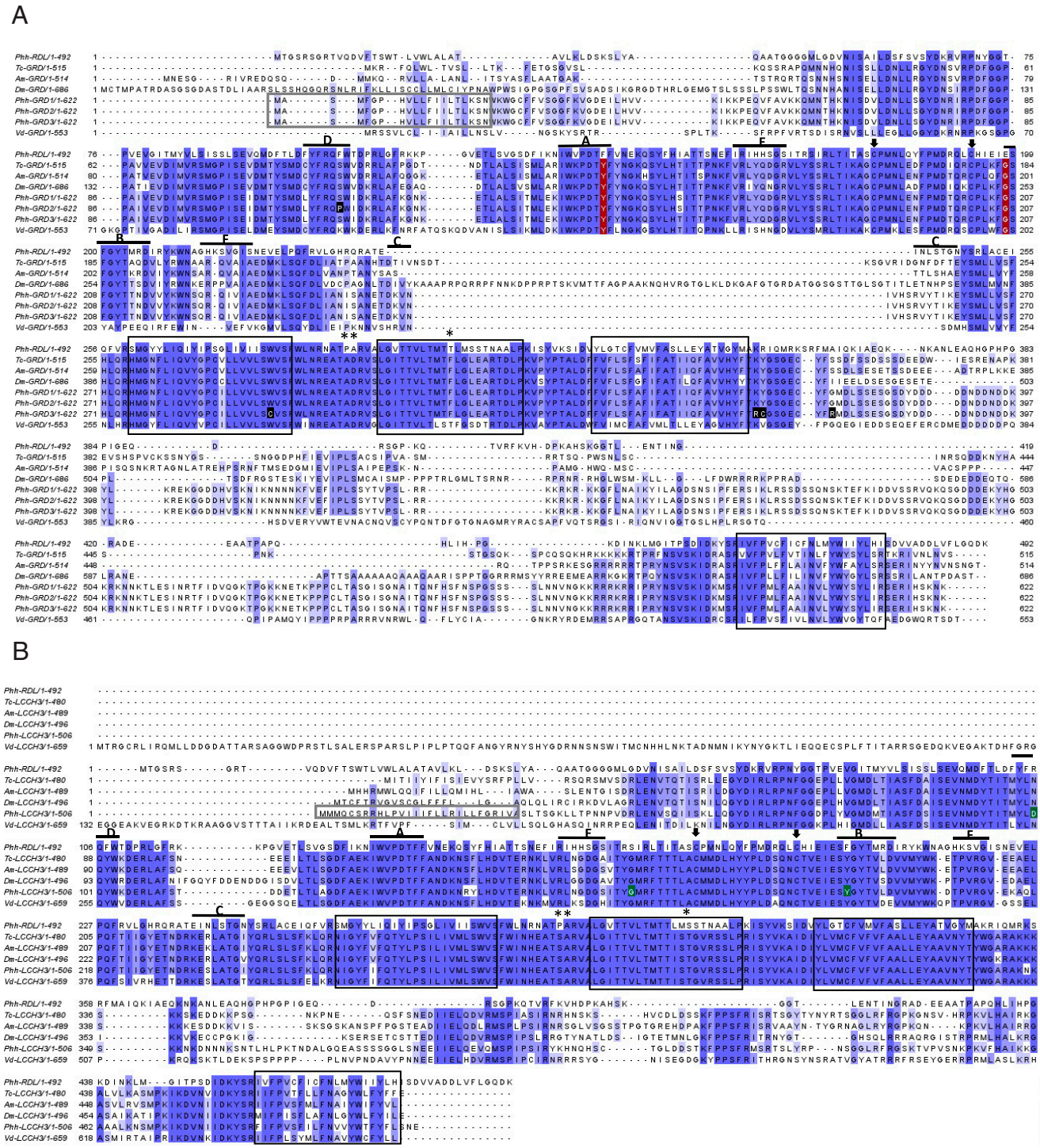

Fig. 2. Multiple sequence alignments conducted in Clustal Omega, then viewed and annotated by Jalview software. (A) Alignment of deduced amino acid sequences of Phh-GRD1, Phh-GRD2, and Phh-GRD3 with the sequences of Vd-GRD (KY748054.1), Am-GRD (NP_001292813.1), Tc-GRD (XP_015834304.1), Dm-GRD (NP_524131.1), and Phh-RDL (QRX38896.1). (B) Alignment of deduced amino acid sequences of Phh-LCCH3 with the sequences of Vd-LCCH3 (KY748055.1), Tc-LCCH3 (NP_001103251.1), Dm-LCCH3 (NP_996469.1), Am-LCCH3 (XP_026298403.1), and Phh-RDL (QRX38896.1). Transmembrane domains (black frames); signal peptides of Phh-GRDs and Phh-LCCH3 (gray frames); C-C loops (arrows); GABA binding loops (A–F, black lines); conserved motifs for ion selectivity (AD at positions –1' and –2' and F at position 13' for Phh-GRDs, SA at positions –1' and –2' and T at position 13' for Phh-LCCH3, asterisks); mutations F148Y and E206G in GABA binding site of Phh-GRD (highlighted in red); mutations R100D, S165G, and F193Y in GABA binding site of Phh-LCCH3 (highlighted in green); and mutation S117P of Phh-GRD2 and mutations W295C, K365R, Y366C, and G374R of Phh-GRD3 (highlighted in black) are indicated.

(UTR) of 75 bp, a CDS of 1771 bp, and a 3′UTR of 23 bp, encoding 622 aa. Phh-GRD was transcribed from the entire open reading frame (ORF) composed of 10 exons and located on contig DS235886 from positions 781055 to 793502 (Fig. 1A). The cloned mRNA sequence of *Phh-lcch3* had 1569 bp with a 5′ UTR of 25 bp, a CDS of 1521 bp, and a 3′ UTR of 23 bp,

encoding 506 aa. The entire ORF of 10 exons was located on contig DS235843 from positions 430552 to 435018 (Fig. 1B).

Sequence and Phylogenetic Analysis of Phh-GRD and Phh-LCCH3. The multiple sequence alignment of deduced aa sequences of Phh-GRD1, Phh-GRD2, and Phh-GRD3 with those well described of other insects/mites revealed that all variants possessed all of the typical features of LGICs: four TM domains, C-C loops, and the signal peptide missing in the putative sequence (Fig. 2A). Sequence analysis showed the presence of AD at positions –1' and –2' (aa 306 and 307) and F at position 13' (aa 321) as indicators of sharp cation selectivity of resulting channel, as described in many reports (Galzi et al., 1992; Corringer et al., 1999; Keramidas et al., 2004; Henry et al., 2020) (Fig. 2A). Phh-GRD2 showed the single mutation S117P in the loop D compared with Phh-GRD1 and Phh-GRD3, whereas Phh-GRD3 revealed mutations W295C (in TM1), K365R, Y366C, and G374R compared with Phh-GRD1 and Phh-GR2. Alignment of deduced aa sequences of the cloned Phh-LCCH3 sequence with those of other insects/mites showed that, as for Phh-GRD, all of the characteristic features of Cys-loop LGICs could be found (Fig. 2B). The aa D was replaced by an R at position 100 located in the GABA binding site of Phh-LCCH3. The presence of SA at positions –1 and –2' (aa 282 and 283) and T at position 13' (aa 301) rendered the Phh-LCCH3 subunit as moderate in terms of ion selectivity in contrast to the sharp anion selectivity of Phh-RDL (QRX38896.1) (Supplemental Fig. 1). Comparison with the Phh-RDL sequence also highlighted some aa differences in the GABA binding site of Phh-GRDs (F148Y-loop A and E206G-loop B) and Phh-LCCH3 (R100D-loop D and S163G and F193Y-loop B) (Supplemental Fig. 1). Sequences of the cloned Phh-GRD1, Phh-GRD2, Phh-GRD3, and Phh-LCCH3 were deposited in NCBI GenBank under the accession numbers OM128123, OM128124, OM128125, and OM128126, respectively.

As expected, phylogenetic analysis revealed that both Phh-GRD and Phh-LCCH3 clustered in separate clades and exhibited closer relationships to their orthologs from relevant organisms rather than other GABA subunits of *P. humanus humanus* (Fig. 3). Phh-GRD showed 67%, 66%, 65%, 60%, and 58% identities with Nv-GRD, Am-GRD, Tc-GRD, Ls-GRD, and Dm-GRD, respectively; whereas Phh-LCCH3 was 81%, 76%, 76%, 73%, and 70% identical to Tc-LCCH3, Am-LCCH3, Ls-LCCH3, Nv-LCCH3, and Dm-LCCH3, respectively. Vd-GRD and Vd-LCCH3 of the mite *V. destructor* were more distant from Phh-GRD and Phh-LCCH3 (46% and 69% identities, respectively).

Expression of *Phh-grd*, *Phh-lcch3*, and *Phh-rdl* along Developmental Stages. To determine the expression levels of *Phh-grd*, *Phh-lcch3*, and *Phh-rdl* in human body louse, mRNA from nits, L1, L2, and L3 larvae stages and adult tissues was extracted and transcribed into cDNA, then submitted to qPCR by using specific primers. *P. humanus humanus β-actin* was used as reference to normalize the expression of the transcripts. It is important to note that the expression of this housekeeping gene, supposed to be stable, was highly variable in the different developmental stages. So, the levels of expression of the subunits could be compared within a stage but not between the stages. Even the differences were not statistically different; Phh-RDL was slightly more expressed than Phh-GRD and Phh-LCCH3 in nits (Fig. 4A), whereas it was the contrary in larvae (Fig. 4B) and in the different tissues of adults (i.e., head, thorax, and abdomen) (Fig. 4C).

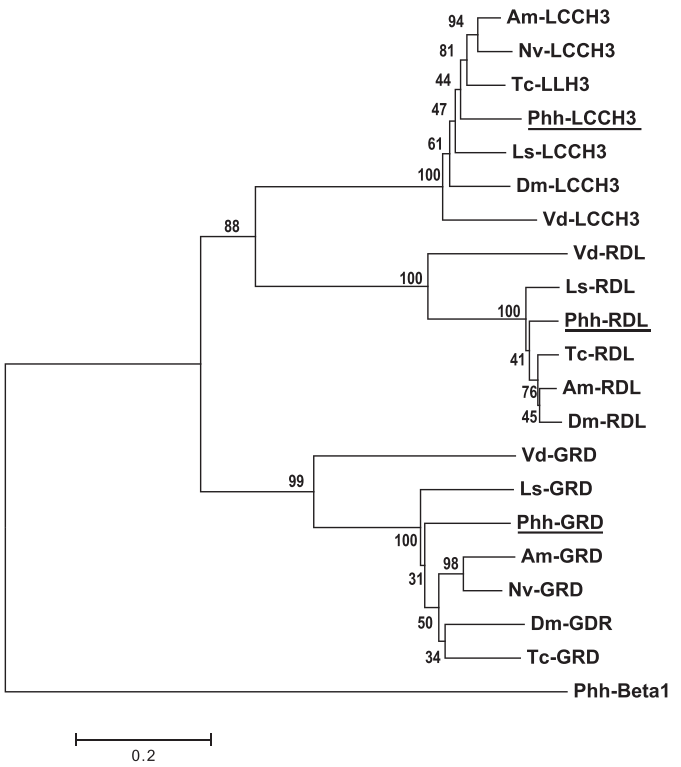

Fig. 3. Evolutionary relationships of *Apis mellifera* Am-LCCH3 (XP_026298403.1); *Drosophila melanogaster* Dm-LCCH3 (NP_996469.1); *Laodelphax striatellus* Ls-LCCH3 (KX355312), *Nasonia vitripennis* Nv-LCCH3 (NP_001234895.1); *Pediculus humanus humanus* Phh-LCCH3 (OM128126); *Tribolium castaneum* Tc-LCCH3 (NP_001103251.1); *Varroa destructor* Vd-LCCH3 (KY748055); Am-GRD (NP_001292813.1); Dm-GRD (NP_524131.1); Ls-GRD (KX355313); Nv-GRD (NP_001234887.1); Phh-GRD (OM128123); Tc-GRD (XP_015834304.1); Vd-GRD (KY748054); Am-RDL (AJE68941); Dm-RDL (NP_523991); Ls-RDL (BAF31884.1); Phh-RDL (QRX38896.1); Tc-RDL (NP_001107809); and Vd-RDL (KY748050). Phh-β1 (unpublished sequence) was used to root the tree. The percentage of replicate trees in which the associated taxa clustered together in the bootstrap test (1050 replicates) are shown next to the branches. The tree is drawn to scale, with branch lengths in the same units as those of the evolutionary distances used to infer the phylogenetic tree. The evolutionary distances were computed using the Poisson correction method and are in the units of the number of amino acid substitutions per site. The analysis involved 21 amino acid sequences. All positions containing gaps and missing data were eliminated. There was a total of 365 positions in the final dataset. Evolutionary analyses were conducted with MEGA7 tool.

Functional Receptors Expressed in *Xenopus laevis* Oocytes. To investigate the functionality of receptors constituted by Phh-GRD and Phh-LCCH3, their respective cRNAs were injected into oocytes of *Xenopus laevis*, and currents in response to GABA were recorded using TEVC. In contrast to Phh-RDL (Lamassiaude et al., 2021), none of the cloned Phh-GRD and Phh-LCCH3 variants was able to constitute a GABA-responsive homomeric receptor. However, Phh-GRD1 was able to reconstitute a functional receptor when coexpressed with Phh-LCCH3, as illustrated by the current traces obtained in response to increasing concentrations of GABA, with the maximum amplitude obtained at 100 μM (Fig. 5A). The $-$log concentration of GABA required to obtain 50% of the maximum response ($-$log EC_{50}) was 5.226 ± 0.012 μM (Fig. 5B). No current was recorded with the application of acetylcholine, glutamate, glycine, aspartate, histamine, and serotonin (Supplemental Fig. 2), indicating that the receptor reconstituted by Phh-GRD1/Phh-LCCH3 is selectively gated by GABA. On the contrary to Phh-GRD1,

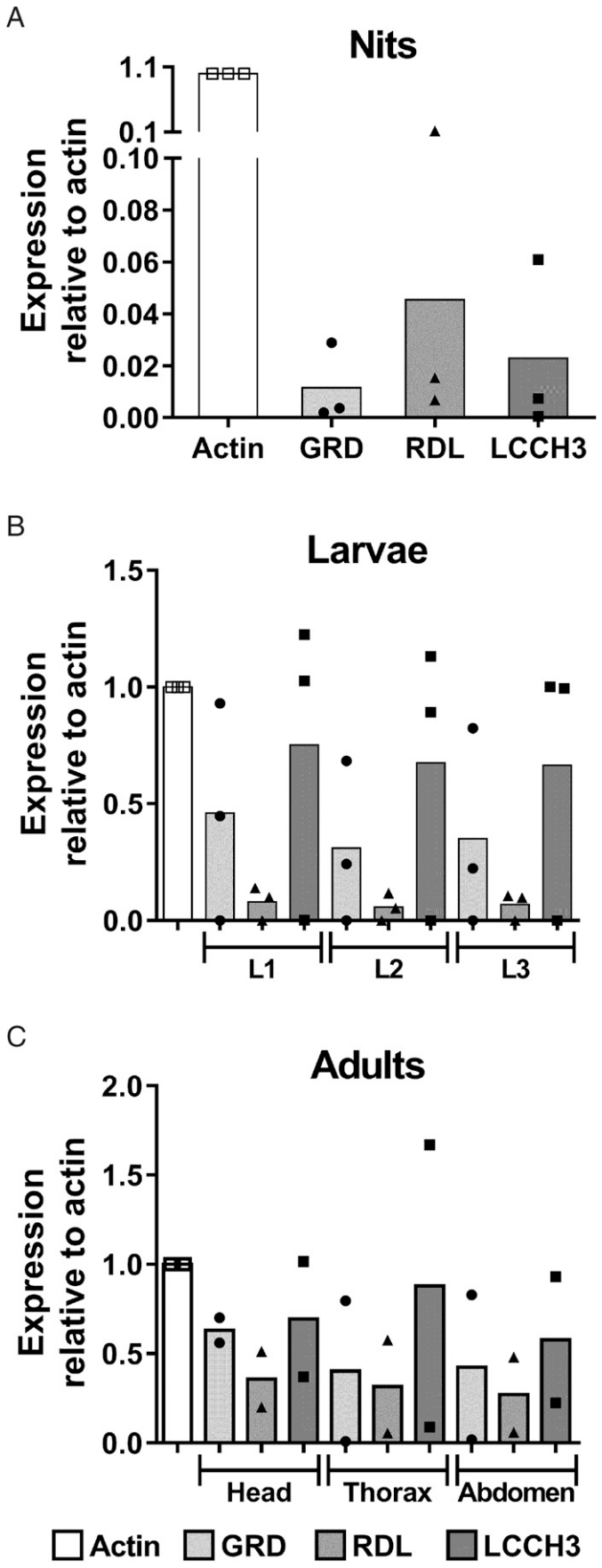

Fig. 4. Relative expression of *Phh-grd, Phh-rdl*, and *Phh-lcch3* throughout the development stages: nits (A); L1, L2, and L3 larvae (B); and in head, thorax, and abdomen of adults (C) of human body louse. Expression of the transcripts was quantified by RT-qPCR, calculated by the comparative Ct method $2^{-(\Delta Ct)}$ and normalized to the expression of actin as endogenous control. The differences between expression of the receptor subunits are not significant (ANOVA test followed by Tukey's multiple comparison test).

Phh-GRD2 and Phh-GRD3 were not able to reconstitute a functional heteromeric receptor with Phh-LCCH3 (Fig. 5C).

It was shown previously by Ménard et al. (2018) that heteromeric GABA receptors could have RDL subunits. We thus tested different Phh-RDL–containing combinations. Both Phh-GRD1/Phh-RDL and Phh-LCCH3/Phh-RDL were functional, as current traces were recorded in the presence of GABA (Fig. 6, A and B). The $-\log EC_{50}$ of 5.076 ± 0.029 μM for Phh-GRD1/Phh-RDL and 5.025 ± 0.032 μM for Phh-LCCH3/Phh-RDL (Fig. 6C) was similar to the $-\log EC_{50}$ of Phh-RDL homomers reconstituted in *Xenopus* oocytes (5.014 ± 0.029 μM; Fig. 6C) but was slightly higher than that calculated for Phh-GRD1/Phh-LCCH3 (5.226 ± 0.012 μM; Fig. 5B).

It is well known that homopentameric receptors constituted by RDL are anion selective, but few reports have categorized the heteropentameric receptors GRD/LCCH3 as cation selective (Gisselmann et al., 2004; Henry et al., 2020). Here we tested the sodium permeability of the heteropentameric receptor Phh-GRD1/Phh-LCCH3. As expected, this receptor was found to be permeable and highly sensitive to the change in the extracellular sodium concentration. Indeed, a shift of 38 mV in reversal potential resulted from changing sodium concentration from 100 to 0 mM (Fig. 6D).

Finally, the antagonist effect of insecticides was studied on Phh-GRD1/Phh-LCCH3. Fipronil and ivermectin were tested at 1 μM, whereas picrotoxin was tested at 10 μM, based on their antagonist effect on Phh-RDL (Lamassiaude et al., 2021). No current was recorded during the preincubation period of 10 seconds before their coapplication with GABA, whereas 10 μM of picrotoxin almost completely abolished the GABA-elicited currents (91.1% ± 2.4% inhibition) and 1 μM fipronil and ivermectin inhibited 72.7% ± 1.1% and 44.7% ± 4.1% of the signal, respectively (Fig. 7A), demonstrating their antagonist effect. In addition, picrotoxin equally antagonized the receptors constituted by Phh-RDL, Phh-GRD1/Phh-LCCH3, Phh-GRD1/Phh-RDL and Phh-LCCH3/Phh-RDL (Fig. 7B). Similarly, fipronil blocked all tested receptors with almost the same potency (70%–80% inhibition of GABA current, Fig. 7C). In contrast, ivermectin antagonized the receptors in the following order: Phh-LCCH3/Phh-RDL > Phh-GRD1/Phh-RDL > Phh-RDL > Phh-GRD1/Phh-LCCH3 (Fig. 7D).

Discussion

In this work, we reported the first molecular, functional, and pharmacological characterization of heteropentameric GABA receptors in the human body louse. By using RT-PCR and RACE-PCR, the complete cDNA of *Phh-grd* and *Phh-lcch3* was cloned, and analysis of the sequences against the putative genes annotated in the database allowed us to redefine the gene organization. Notably, results of 3′ RACE for *Phh-grd* exhibited retention of a part of intron 7 and the whole intron 8 located between TM3 and TM4 of the intracellular domain, as for *Vd-grd* (Ménard et al., 2018). Since these

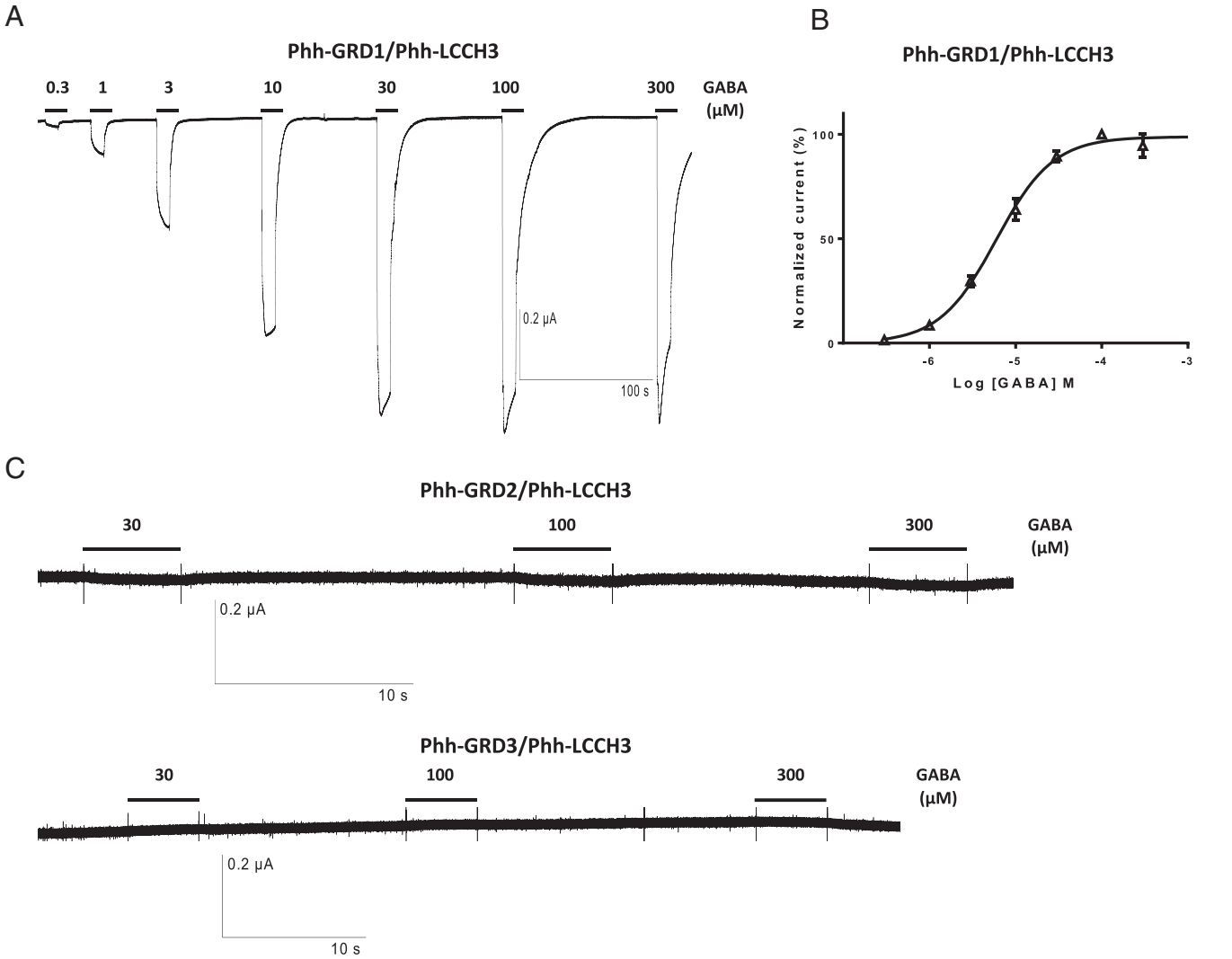

Fig. 5. Functional expression of Phh-GRD1/Phh-LCCH3 but not of Phh-GRD2-3/Phh-LCCH3 receptors in *X. laevis* oocytes. (A) Current trace obtained on oocytes injected with cRNA of Phh-GRD1/Phh-LCCH3 in response to GABA in the range of 0.3–300 μM. Oocytes were clamped at −60 mV. Application time of 10 seconds is indicated by the bars. (B) GABA concentration response curve for Phh-GRD1/Phh-LCCH3 (n = 17 oocytes). Data were normalized to the maximal effect obtained by 100 μM GABA. (C) Means ± S.D. of representative current traces obtained on oocytes coinjected with Phh-GRD2/Phh-LCCH3 (n = 13) and Phh-GRD3/Phh-LCCH3 (n = 15) in response to 30–300 μM GABA. Oocytes were clamped at −60 mV. Application time of 5 seconds is indicated by the bars.

sequences were obtained in all clones and further confirmed by the transcriptomics project (unpublished data), we hypothesize that it would be a wrong annotation of the genome rather than intron retentions. Results of 5′ RACE of *Phh-grd* revealed an insertion of 54 aa at the N-terminal domain before the C-C loop. Similar insertions were described in *Vd-grd* (Ménard et al., 2018) and *Dm-grd* (Harvey et al., 1994), but these insertions are not identical and seem to be species specific. Interestingly, two in-frame methionine residues were found at the 5′ end of all cloned variants of *Phh-grd*, and this is in agreement with what was described in transcripts encoding many membrane-associated proteins in *Drosophila* (Harvey et al., 1994).

None of the Phh-GRDs and Phh-LCCH3 subunits was able to reconstitute homomeric functional receptor, in agreement with the results obtained with these subunits of *D. melanogaster*, *A. mellifera*, and *V. destructor* (Gisselmann et al., 2004; Ménard et al., 2018; Henry et al., 2020). Compared with Phh-RDL, able to form homomeric receptors functional in *Xenopus* oocytes (Lamassiaude et al., 2021), aa modifications F148Y/E206G and R100D/S163G/F193Y (Supplemental Fig. 1) were identified in the GABA binding site of Phh-GRD and Phh-LCCH3, respectively. As these aa belong to the seven aa assumed to be essential for the binding of GABA described in Dm-RDL and Am-RDL (Ashby et al., 2012; Henry et al., 2020), the lack of current upon GABA application is not surprising. When assembled together, Phh-GRD and Phh-LCCH3 respond to GABA, suggesting that the two subunits constitute a heteromeric receptor with functional GABA binding site. We can so hypothesize that the aa modifications in the GABA binding site of one subunit were complemented by the corresponding aa of the other subunit. Indeed, it has been shown that Am-GRD and Am-LCCH3 were able to respond to GABA as heteromeric receptor in spite of a tyrosine at the position 182 of Am-LCCH3 (Henry et al., 2020). The variant Phh-GRD2 was unable to form a functional heteromeric receptor with Phh-LCCH3. It seems that the proline at position 117 was not able to preserve the functionality of serine and was not complemented by the corresponding position of Phh-LCCH3.

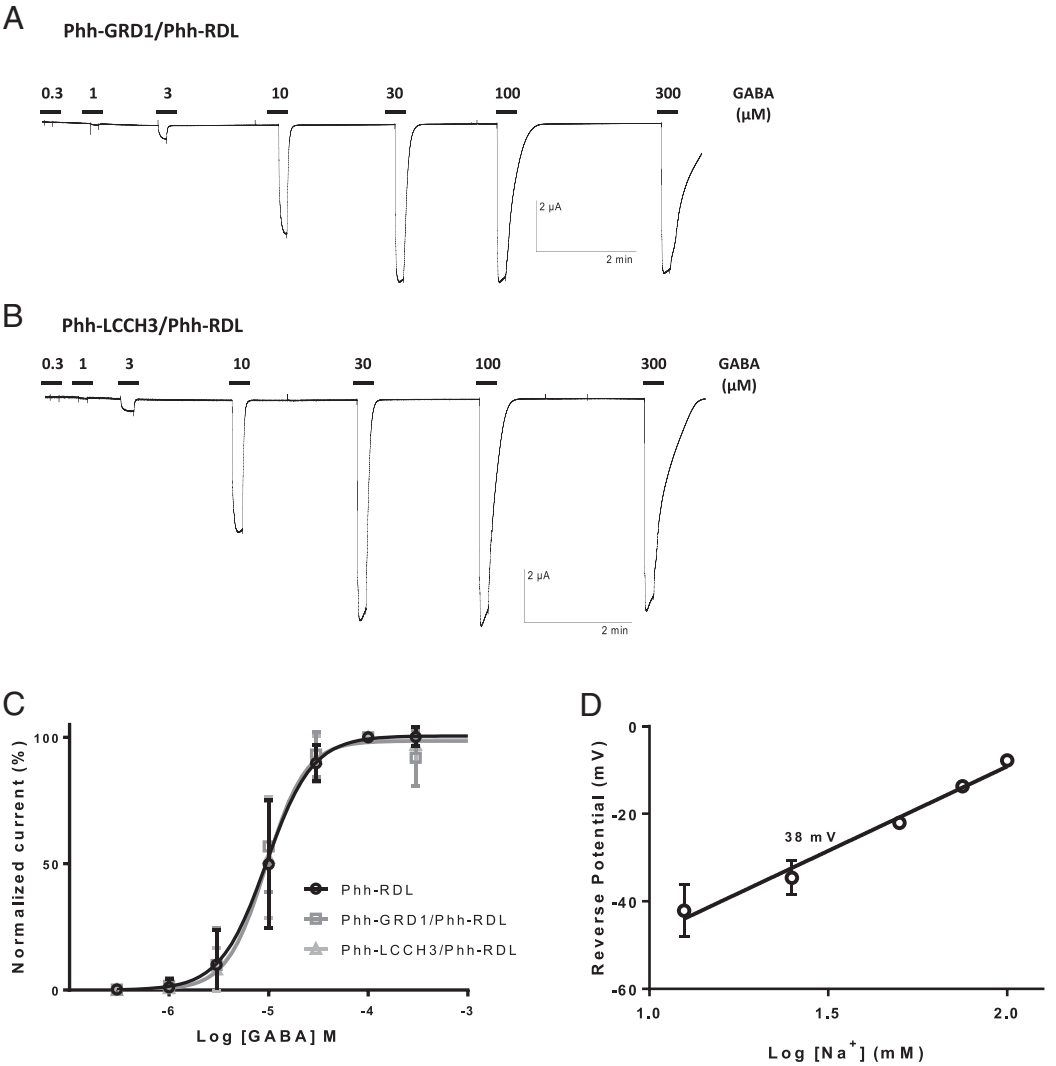

Fig. 6. Functional expression of Phh-GRD1/Phh-RDL and Phh-LCCH3/Phh-RDL receptors in *X. laevis* oocytes. Current trace obtained on oocytes injected with cRNA of Phh-GRD1/Phh-RDL (A) and Phh-LCCH3/Phh-RDL (B) in response to GABA in the range of 0.3–300 μM. Oocytes were clamped at −60 mV. Application time of 10 seconds is indicated by the black bar. (C) Means ± S.D. of GABA concentration-response curves for Phh-RDL, Phh-GRD1/Phh-RDL, and Phh-LCCH3/Phh-RDL (n = 20, n = 9, n = 7 oocytes, respectively). Data were normalized to the maximal effect obtained with 100 μM GABA. (D) Reverse potential ion-concentration relationship (means ± S.D.) for sodium ions of Phh-GRD/Phh-LCCH3–expressing oocytes in the presence of 100 μM GABA and decreasing concentrations of Na^+ (100 to 0 mM).

For Phh-GRD3, one or more of the mutations W295C, K365R, Y366C, and G374R might be responsible for the nonfunctionality of Phh-GRD3/Phh-LCCH3. The mutation W295C is located in TM1 and the other mutations are in the highly variable intracellular area between TM3 and TM4, but data of the literature on mutations in the different TM domains of RDL give contradictory information on their importance in the functionality of GABA receptor. On one hand, Phh-RDL2, unable to form a functional receptor, differed from the functional variant Phh-RDL by only 20 amino acids, among them a mutation in TM1 (D281V) that could be responsible for its nonresponsiveness to GABA in *Xenopus* oocytes (Lamassiaude et al., 2021). On the other hand, *Cyrtorhinus lividipennis* RDL with an insertion of 31 aa between TM3 and TM4 was much less sensitive to fipronil than the RDL without insertion (Jiang et al., 2015). Finally, no important difference in response to GABA, imidacloprid, and fipronil has been shown between Am-RDL variants with variable sequences in TM3 and TM4 (Taylor-Wells et al., 2017).

Sodium permeability of the receptor Phh-GRD1/Phh-LCCH3 was confirmed by recording change in reversal potential with decreasing concentrations of sodium and high sensitivity of the resulting channel to changes in Na^+ concentration (Fig. 6D). In *A. mellifera*, Am-LCCH3/Am-RDL constituted anion-selective channel, whereas Am-GRD/Am-LCCH3 was cation selective (Henry et al., 2020). The existence of aa AD at positions –1' and –2' and F at position 13' of Phh-GRD is a good indicator for cation selectivity of the heteromeric receptor Phh-GRD/Phh-LCH3. The same motifs were described in Dm-GRD, Vd-GRD, and Am-GRD, and the cation selectivity of GRD/LCCH3 receptors of the three organisms was confirmed by electrophysiology (Gisselmann et al., 2004; Ménard et al., 2018; Henry et al., 2020). This cation selectivity filter was also described in LGICs of other organisms, such as EXP-1 of *Caenorhabditis elegans* and 5HT3 and alpha 7 subunit of nACh receptor (nAChRα7) of rat (Corringer et al., 1999; Wotring et al., 2003). Interestingly, the introduction of three aa into the TM2 segment of nAChRα7

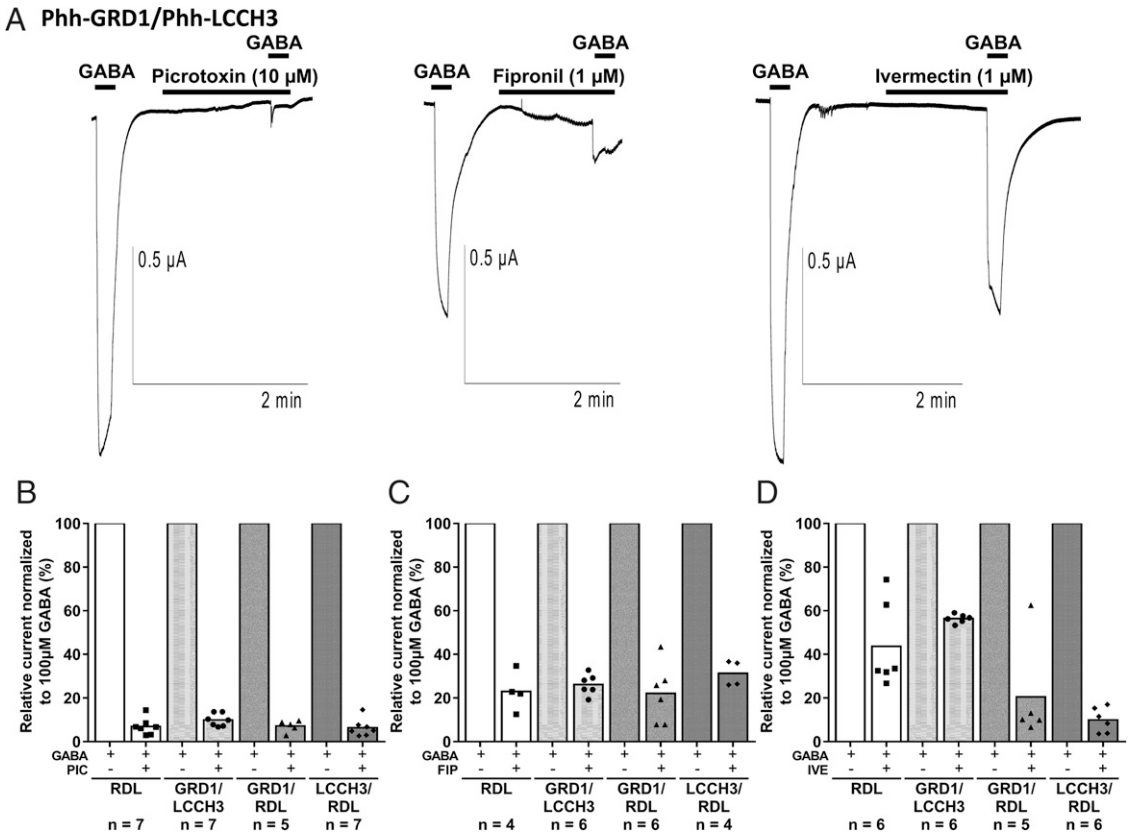

Fig. 7. Antagonistic effects of fipronil, picrotoxin, and ivermectin on GABA receptors expressed in *X. laevis* oocytes. Representative current traces from single oocyte expressing Phh-GRD1/Phh-LCCH3 receptor alone or with coapplication of 10 μM picrotoxin, 1 μM fipronil, and 1 μM ivermectin (A). Relative current evoked by 100 μM GABA alone (=100%) or with coapplication of 10 μM picrotoxin (PIC, B); 1 μM fipronil (FIP, C); and 1 μM ivermectin (IVE, D) on oocytes expressing Phh-RDL, Phh-GRD1/Phh-LCCH3, Phh-GRD1/Phh-RDL, and Phh-LCCH3/Phh-RDL (n = 4–7, as indicated on each figure). No significant differences ($P > 0.05$) were calculated between the results of the different receptors with picrotoxin (PIC, B) or fipronil (FIP, C), whereas P value = 0.0048 for Phh-RDL vs. Phh-LCCH3/Phh-RDL and for Phh-GRD1/Phh-LCCH3 vs. Phh-GRD1/Phh-RDL and P value = 0.0002 for Phh-GRD1/Phh-LCCH3 vs. Phh-LCCH3/Phh-RDL with 1 μM ivermectin (IVE, D) (one-way ANOVA followed by Tukey's multiple comparisons test).

converted the cation-selective channel into an anion-selective channel gated by acetylcholine (Galzi et al., 1992). The presence of motifs SA at positions –1' and –2' and T at position 13' (Fig. 2B) marks Phh-LCCH3 as intermediate in terms of ion selectivity, meaning that the global anion selectivity of the heteromeric receptor is determined by the Phh-GRD subunit. In honey bee, Am-LCCH3/Am-RDL constituted anion-selective channel, whereas Am-LCCH3/Am-GRD was cation selective (Henry et al., 2020).

The Phh-GRD1/Phh-LCCH3 heteromeric receptor responded to GABA in a concentration-dependent manner with slightly higher sensitivity to GABA than the prototype homomeric Phh-RDL but with almost the same GABA sensitivity as Dm-GRD/Dm-LCCH3 and Am-GRD/Am-LCCH3 (Gisselmann et al., 2004; Henry et al., 2020). The EC_{50} calculated for the receptor Vd-GRD/Vd-LCCH3 of the mite *V. destructor* was much more elevated (35 μM) (Ménard et al., 2018). Absence of current in response to other potential ligands confirmed selectivity of Phh-GRD1/Phh-LCCH3 toward GABA. To our knowledge, the heteromer GRD/RDL had not been investigated in insects up until now. In the present study, there was no important difference in response to GABA between the homomer Phh-RDL and the heteromers Phh-GRD1/Phh-RDL and Phh-LCCH3/Phh-RDL, but heteromeric receptors with similar EC_{50} could have distinct pharmacology. It is not possible to affirm that Phh-GRD1/Phh-RDL and Phh-LCCH3/Phh-RDL are really reconstituted by both subunits and not by Phh-RDL alone. Their higher sensitivity toward ivermectin is in favor of this hypothesis; however, assays like immune coprecipitation are required to confirm the existence of heteromers. It has been shown that the coexpression of LCCH3 could alter the pharmacological properties of the RDL receptor. For example, Dm-RDL was picrotoxin sensitive and bicuculline insensitive, whereas Dm-RDL/Dm-LCCH3 was picrotoxin insensitive and bicuculline sensitive (Zhang et al., 1995). Interestingly, lower IC_{50} for fluralaner and fipronil but higher IC_{50} for dieldrin were observed in blocking GABA-activated current when two variants of *C. suppressalis* RDL were coexpressed in *Xenopus* oocytes than when each variant was expressed individually (Sheng et al., 2018). This points out the fact that reconstitution of receptors with different variants of the same subunit further complicates the expression profile of GABA receptors in arthropods.

Concerning in situ expression, *Dm-rdl* and *Dm-lcch3* were not found in the same tissues of the nervous system of *Drosophila* (Aronstein et al., 1996). These two subunits were assembled and functional in *Xenopus* oocytes, indicating that the functionality of GABA receptors in this heterologous expression system does not systematically imply their existence

in vivo. In the case of *Phh-grd, Phh-rdl*, and *Phh-lcch3*, results of relative expression showed that the three subunits were present in all developmental stages and in the different parts of the adults (head, thorax, and abdomen). Similar results were observed in *L. striatellus, C. suppressalis*, and *A. mellifera*, where *grd*, *lcch3*, or *rdl* subunits were detected during the whole life cycle and in different parts of the insects (Wei et al., 2017; Jia et al., 2019; Henry et al., 2020), but mainly in larvae of *D. melanogaster* (Knipple and Soderlund, 2010), whereas *rdl* was essentially found in the head of *Musca domestica* (Kita et al., 2019). The relatively similar expression pattern of *Phh-grd* and *Phh-lcch3* during developmental stages and in different parts could explain their tendency to form heteromeric cation-selective receptors that could play an important physiologic role in the nervous system of human louse, one of them being their role as excitatory mediators during developmental stages of neuronal wiring or under pathologic conditions (Henry et al., 2020). Fipronil and ivermectin antagonized all receptors tested here and killed human lice (Lamassiaude et al., 2021). Relationship between receptor targeting and pediculicide activity could be confirmed using RNA interference (RNAi) strategy as shown for *L. striatellus*, in which injection of *rdl* double-stranded RNA (dsRNA) reduced fipronil-induced mortality (Wei et al., 2015).

In summary, this work allowed us to clone and characterize *Phh-grd* and *Phh-lcch3* subunits of GABA receptors from human body louse. These results revealed that *Phh-grd, Phh-lcch3*, and *Phh-rdl* were expressed throughout the developmental stages and in different tissues. At the functional level, heteromeric receptors constituted by Phh-GRD1/Phh-LCCH3, Phh-GRD1/Phh-RDL, and Phh-LCCH3/Phh-RDL were able to respond to GABA in a concentration-dependent manner with variable sensitivities to picrotoxin, fipronil, and ivermectin. Altogether, these findings provide major basis for future investigations on LGICs to understand the mechanisms of action of pediculicides as well as their roles in resistance to insecticides.

Acknowledgments

The authors thank Nancy Jabbour for her participation in the cloning of *Phh-lcch3* during her master internship.

Authorship Contributions

Participated in research design: Hashim, Charvet, Neveu, Dimier-Poisson, Debierre-Grockiego, Dupuy.

Conducted experiments: Hashim, Charvet, Toubaté, Lamassiaude, Dupuy.

Performed data analysis: Hashim, Charvet, Debierre-Grockiego, Dupuy.

Wrote or contributed to the writing of the manuscript: Hashim, Charvet, Ahmed, Neveu, Dimier-Poisson, Debierre-Grockiego, Dupuy.

References

Amanzougaghene N, Fenollar F, Raoult D, and Mediannikov O (2020) Where are we with human lice? A review of the current state of knowledge. *Front Cell Infect Microbiol* **9**:474.

Antinori S, Mediannikov O, Corbellino M, Grande R, Parravicini C, Bestetti G, Longhi E, Ricaboni D, Ehounoud CB, Fenollar F, et al. (2016) Louse-borne relapsing fever (*Borrelia recurrentis*) in a Somali refugee arriving in Italy: a re-emerging infection in Europe? *PLoS Negl Trop Dis* **10**:e0004522.

Aronstein K, Auld V, and Ffrench-Constant R (1996) Distribution of two GABA receptor-like subunits in the *Drosophila* CNS. *Invert Neurosci* **2**:115–120.

Ashby JA, McGonigle IV, Price KL, Cohen N, Comitani F, Dougherty DA, Molteni C, and Lummis SCR (2012) GABA binding to an insect GABA receptor: a molecular dynamics and mutagenesis study. *Biophys J* **103**:2071–2081.

Badiaga S and Brouqui P (2012) Human louse-transmitted infectious diseases. *Clin Microbiol Infect* **18**:332–337.

Bechah Y, Capo C, Mege J-L, and Raoult D (2008) Epidemic typhus. *Lancet Infect Dis* **8**:417–426.

Buckingham SD, Biggin PC, Sattelle BM, Brown LA, and Sattelle DB (2005) Insect GABA receptors: splicing, editing, and targeting by antiparasitics and insecticides. *Mol Pharmacol* **68**:942–951.

Clark JM, Yoon KS, Lee SH, and Pittendrigh BR (2013) Human lice: past, present and future control. *Pestic Biochem Physiol* **106**:162–171 DOI: 10.1016/j.pestbp.2013.03.008

Corringer PJ, Bertrand S, Galzi JL, Devillers-Thiéry A, Changeux JP, and Bertrand D (1999) Mutational analysis of the charge selectivity filter of the alpha7 nicotinic acetylcholine receptor. *Neuron* **22**:831–843.

DE LA Filia AG, Andrewes S, Clark JM, and Ross L (2018) The unusual reproductive system of head and body lice (*Pediculus humanus*). *Med Vet Entomol* **32**:226–234.

Galzi JL, Devillers-Thiéry A, Hussy N, Bertrand S, Changeux JP, and Bertrand D (1992) Mutations in the channel domain of a neuronal nicotinic receptor convert ion selectivity from cationic to anionic. *Nature* **359**:500–505.

Gisselmann G, Plonka J, Pusch H, and Hatt H (2004) *Drosophila melanogaster* GRD and LCCH3 subunits form heteromultimeric GABA-gated cation channels. *Br J Pharmacol* **142**:409–413.

Harvey RJ, Schmitt B, Hermans-Borgmeyer I, Gundelfinger ED, Betz H, and Darlison MG (1994) Sequence of a *Drosophila* ligand-gated ion-channel polypeptide with an unusual amino-terminal extracellular domain. *J Neurochem* **62**:2480–2483.

Henry C, Cens T, Charnet P, Cohen-Solal C, Collet C, van-Dijk J, Guiramand J, de Jésus-Ferreira M-C, Menard C, Mokrane N, et al. (2020) Heterogeneous expression of GABA receptor-like subunits LCCH3 and GRD reveals functional diversity of GABA receptors in the honeybee *Apis mellifera*. *Br J Pharmacol* **177**:3924–3940.

Hoch M, Wieser A, Löscher T, Margos G, Pürner F, Zühl J, Seilmaier M, Balzer L, Guggemos W, Rack-Hoch A, et al. (2015) Louse-borne relapsing fever (*Borrelia recurrentis*) diagnosed in 15 refugees from northeast Africa: epidemiology and preventive control measures, Bavaria, Germany, July to October 2015. *Euro Surveill* **20**.

Huang QT, Sheng CW, Jones AK, Jiang J, Tang T, Han ZJ, and Zhao CQ (2021) Functional characteristics of the lepidopteran ionotropic GABA receptor 8916 subunit interacting with the LCCH3 or the RDL subunit. *J Agric Food Chem* **69**:11582–11591.

Hytönen J, Khawaja T, Grönroos JO, Jalava A, Meri S, and Oksi J (2017) Louse-borne relapsing fever in Finland in two asylum seekers from Somalia. *APMIS* **125**:59–62.

Jia Z-Q, Sheng C-W, Tang T, Liu D, Leviticus K, Zhao C-Q, and Chang X-L (2019) Identification of the ionotropic GABA receptor-like subunits from the striped stem borer, *Chilo suppressalis* Walker (Lepidoptera: Pyralidae). *Pestic Biochem Physiol* **155**:36–44.

Jiang F, Zhang Y, Sun H, Meng X, Bao H, Fang J, and Liu Z (2015) Identification of polymorphisms in *Cyrtorhinus lividipennis* RDL subunit contributing to fipronil sensitivity. *Pestic Biochem Physiol* **117**:62–67.

Johnson-Arbor K (2022) Ivermectin: a mini-review. *Clin Toxicol (Phila)* **60**:571–575.

Jones AK, Goven D, Froger J-A, Bantz A, and Raymond V (2021) The cys-loop ligand-gated ion channel gene superfamilies of the cockroaches *Blattella germanica* and *Periplaneta americana*. *Pest Manag Sci* **77**:3787–3799.

Keramidas A, Moorhouse AJ, Schofield PR, and Barry PH (2004) Ligand-gated ion channels: mechanisms underlying ion selectivity. *Prog Biophys Mol Biol* **86**:161–204.

Kita T, Mino H, Ozoe F, and Ozoe Y (2019) Spatiotemporally different expression of alternatively spliced GABA receptor subunit transcripts in the housefly *Musca domestica*. *Arch Insect Biochem Physiol* **101**:e21541.

Knipple DC and Soderlund DM (2010) The ligand-gated chloride channel gene family of *Drosophila melanogaster*. *Pestic Biochem Physiol* **97**:140–148 DOI: 10.1016/j.pestbp.2009.09.002.

Kozuska JL and Paulsen IM (2012) The Cys-loop pentameric ligand-gated ion channel receptors: 50 years on. *Can J Physiol Pharmacol* **90**:771–782.

Kumar S, Stecher G, and Tamura K (2016) MEGA7: Molecular Evolutionary Genetics Analysis Version 7.0 for bigger datasets. *Mol Biol Evol* **33**:1870–1874.

Lamassiaude N, Toubate B, Neveu C, Charnet P, Dupuy C, Debierre-Grockiego F, Dimier-Poisson I, and Charvet CL (2021) The molecular targets of ivermectin and lotilaner in the human louse *Pediculus humanus humanus*: new prospects for the treatment of pediculosis. *PLoS Pathog* **17**:e1008863.

Madeira F, Park YM, Lee J, Buso N, Gur T, Madhusoodanan N, Basutkar P, Tivey ARN, Potter SC, Finn RD, et al. (2019) The EMBL-EBI search and sequence analysis tools APIs in 2019. *Nucleic Acids Res* **47**:W636–W641.

Ménard C, Folacci M, Brunello L, Charreton M, Collet C, Mary R, Rousset M, Thibaud J-B, Vignes M, Charnet P, et al. (2018) Multiple combinations of RDL subunits diversify the repertoire of GABA receptors in the honey bee parasite *Varroa destructor*. *J Biol Chem* **293**:19012–19024.

Mohammadi J, Azizi K, Alipour H, Kalantari M, Bagheri M, Shahriari-Namadi M, Ebrahimi S, and Moemenbellah-Fard MD (2021) Frequency of pyrethroid resistance in human head louse treatment: systematic review and meta-analysis. *Parasite* **28**:86.

Olds BP, Coates BS, Steele LD, Sun W, Agunbiade TA, Yoon KS, Strycharz JP, Lee SH, Paige KN, Clark JM, et al. (2012) Comparison of the transcriptional profiles of head and body lice. *Insect Mol Biol* **21**:257–268.

Osthoff M, Schibli A, Fadini D, Lardelli P, and Goldenberger D (2016) Louse-borne relapsing fever - report of four cases in Switzerland, June-December 2015. *BMC Infect Dis* **16**:210.

Petersen TN, Brunak S, von Heijne G, and Nielsen H (2011) SignalP 4.0: discriminating signal peptides from transmembrane regions. *Nat Methods* **8**:785–786.

Sallard E, Letourneur D, and Legendre P (2021) Electrophysiology of ionotropic GABA receptors. *Cell Mol Life Sci* **78**:5341–5370.

Sangaré AK, Doumbo OK, and Raoult D (2016) Management and treatment of human lice. *BioMed Res Int* **2016**:8962685.
Sheng C-W, Jia Z-Q, Ozoe Y, Huang Q-T, Han Z-J, and Zhao C-Q (2018) Molecular cloning, spatiotemporal and functional expression of GABA receptor subunits RDL1 and RDL2 of the rice stem borer *Chilo suppressalis*. *Insect Biochem Mol Biol* **94**:18–27.
Taylor-Wells J, Hawkins J, Colombo C, Bermudez I, and Jones AK (2017) Cloning and functional expression of intracellular loop variants of the honey bee (*Apis mellifera*) RDL GABA receptor. *Neurotoxicology* **60**:207–213.
Tong G, Baker MA, and Shenvi RA (2021) Change the channel: CysLoop receptor antagonists from nature. *Pest Manag Sci* **77**:3650–3662.
Wei Q, Wu S-F, and Gao C-F (2017) Molecular characterization and expression pattern of three GABA receptor-like subunits in the small brown planthopper *Laodelphax striatellus* (Hemiptera: Delphacidae). *Pestic Biochem Physiol* **136**:34–40.
Wei Q, Wu S-F, Niu C-D, Yu H-Y, Dong Y-X, and Gao C-F (2015) Knockdown of the ionotropic γ-aminobutyric acid receptor (GABAR) RDL gene decreases fipronil susceptibility of the small brown planthopper, *Laodelphax striatellus* (Hemiptera: Delphacidae). *Arch Insect Biochem Physiol* **88**:249–261.
Wilting KR, Stienstra Y, Sinha B, Braks M, Cornish D, and Grundmann H (2015) Louse-borne relapsing fever (*Borrelia recurrentis*) in asylum seekers from Eritrea, the Netherlands, July 2015. *Euro Surveill* **20**:21196.
Wotring VE, Miller TS, and Weiss DS (2003) Mutations at the GABA receptor selectivity filter: a possible role for effective charges. *J Physiol* **548**:527–540.
Zhang HG, Lee HJ, Rocheleau T, ffrench-Constant RH, and Jackson MB (1995) Subunit composition determines picrotoxin and bicuculline sensitivity of Drosophila gamma-aminobutyric acid receptors. *Mol Pharmacol* **48**:835–840.

Address correspondence to: Dr. Catherine Dupuy, Unité Mixte de Recherche Université de Tours, INRAE 1282 ISP, BioMAP, Faculté de Pharmacie, 31 avenue Monge, 37200 Tours, France. E-mail: catherine.dupuy@univ-tours.fr